molecular pharmaceutics

Brief Article

pubs.acs.org/molecularpharmaceutics

Curcumin/Gd Loaded Apoferritin: A Novel "Theranostic" Agent To Prevent Hepatocellular Damage in Toxic Induced Acute Hepatitis

Juan Carlos Cutrin,[†,‡] Simonetta Geninatti Crich,[*,†] Diana Burghelea,[†] Walter Dastrù,[†] and Silvio Aime[†]

[†]Department of Molecular Biotechnology and Health Sciences, University of Torino, via Nizza 52, 10126, Torino, Italy

[‡]ININCA-CONICET, Marcelo T De Alvear 2270, CP122, AAJ, Buenos Aires, Argentina

Supporting Information

ABSTRACT: Apoferritin has been exploited to deliver simultaneously therapeutic and imaging agents (loaded into its internal cavity) to hepatocytes as this protein is efficiently taken up from blood by hepatocyte scavenger receptor class A type 5 via the ferritin transporting route. To this purpose the protein has been loaded with the magnetic resonance imaging (MRI) contrast agent GdHPDO3A and curcumin, a polyphenolic substance endowed with multiple pharmacological actions, namely: antioxidant, anti-inflammatory, antineoplastic. Curcumin and GdHPDO3A loaded apoferritin has been used with the aim to attenuate the thioacetamide-induced hepatitis together with the evaluation by MRI of drug delivery efficiency. Mice pretreated by intraperitoneal administration showed significantly attenuated hepatic injury as assessed by measuring alanine aminotransferase (ALT) activity in plasma and by histology assessment. The encapsulation of curcumin inside the apoferritin cavity significantly increases its stability and bioavailability while maintaining its therapeutic anti-inflammatory properties.

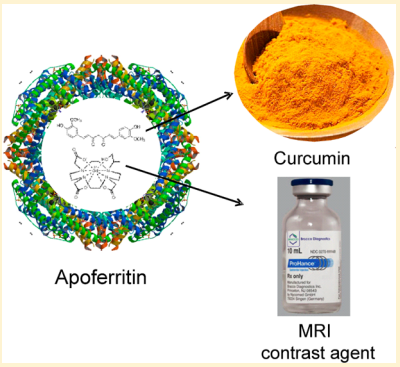

KEYWORDS: *curcumin, apoferritin, MRI, Gd(III), hepatitis*

INTRODUCTION

Apoferritin is an excellent carrier to deliver drugs to hepatocytes as it is efficiently taken up from blood by hepatocyte scavenger receptor class A type 5 (SCARA 5).[1] Moreover, the amount of apoferritin taken-up can be quantitatively visualized when the protein is loaded with a magnetic resonance imaging (MRI) contrast agent such as Gd-HPDO3A.[2] The loading procedure consists of lowering the pH of the apoferritin containing solution followed by the addition of the solutes to be uploaded. The supramolecular structure of apoferritin collapses because of the break of the electrostatic interactions that maintain its spherical hollow structure. The pH is then returned to 7 in order to restore the spherical supramolecular shape of apoferritin, now entrapping the desired solutes in its inner cavity. Thus, upon entrapping therapeutic and imaging molecules into apoferritin, a general liver "theranostic" agent[3] can be attained. The use of these nanotheranostic agents permit to analyze noninvasively the pharmacokinetic and biodistribution of the nanomedicine formulation, by following in real time the efficacy of the therapy and thereby to adapt the treatment regimens on the basis of biodistribution and efficacy monitoring.

Herein, the preparation and "in vivo" testing of curcumin and Gd-HPDO3A loaded apoferritin (Apo-CUR-Gd, Scheme 1) is reported. Curcumin, a polyphenolic (diferuloylmethane) substance, is the main yellow pigment extracted from the turmeric *Curcuma longa*.[4] Curcumin is a versatile bioactive compound possessing multiple pharmacological actions namely: antioxidant, anti-inflammatory, antihyperlipidemic, liver antifibrotic, antiangiogenic, antineoplastic, and chemoprotective.[5] Although clinical trials have demonstrated the safety of curcumin even at high doses (12 g/day),[6] the clinical translation of this promising natural compound is hampered by its poor water solubility and short biological half-life, resulting in low (micromolar range) bioavailability in both plasma and tissues. In order to improve the bioavailability of curcumin, several approaches have been employed including the combination of curcumin with adjuvants[7] (e.g., piperine, rubusoside), and the development of delivery vehicles[8] consisting of liposomes, nanoparticles, and phospholipid formulations.

EXPERIMENTAL SECTION

Gd-HPDO3A (Prohance) was kindly provided by Bracco Imaging S.p.A (Milan, Italy). Apoferritin (from equine spleen), thioacetamide, and all other chemicals were purchased from Sigma-Aldrich (St. Louis, MO). The R_1 nuclear magnetic relaxation dispersion profiles of water protons were measured over a continuum of magnetic field strengths from 0.00024 to 0.5 T (corresponding to 0.01−20 MHz proton Larmor frequencies) on a fast field-cycling Stelar Spinmaster FFC 2000 relaxometer [Stelar S.n.c., Mede (PV), Italy] equipped with a silver magnet. The relaxometer operated under complete computer control with an absolute uncertainty in the R_1 values of ±1%. Water proton T_1 measurements at fixed frequency were carried out on a

Received: October 26, 2012
Revised: March 25, 2013
Accepted: April 2, 2013
Published: April 2, 2013

Scheme 1. Schematic Representation of Apo-CUR-Gd Preparation and of Both the Diagnostic (Gd-HPDO3A) and Therapeutic (Curcumin) Probes Loaded in the Apoferritin Cavity

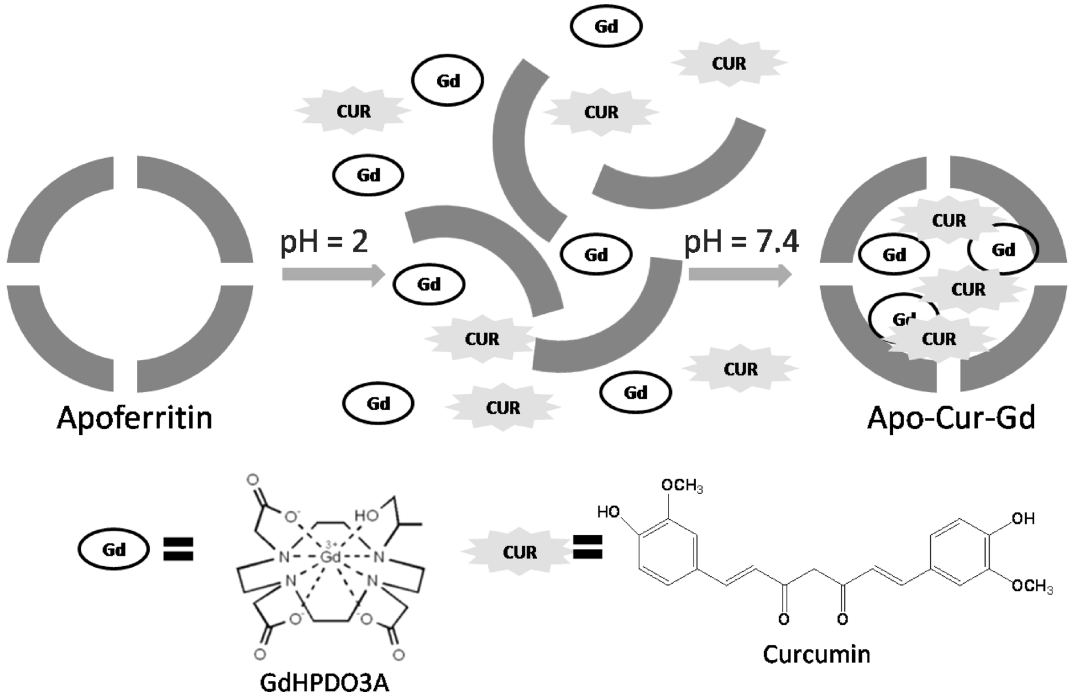

Stelar SpinMaster spectrometer operating in the range from 20 to 80 MHz, by means of the inversion–recovery method (16 experiments, two scans). The reproducibility of the T_1 data was ±0.5%.

Apo-CUR-Gd Preparation. The loading of curcumin and Gd-HPDO3A in the apoferritin cavity was carried out as described previously[1]. Briefly, the dissociation of the apoferritin into its subunits was done by lowering the pH of the protein solution (1×10^{-5} mol/L) down to pH 2 using HCl 1 M and maintaining this low pH for about 15 min. Afterward, 5 μL of a curcumin solution in DMSO (200 mg/mL) and 0.2 mL Gd-HPDO3A 0.5 M have been added for every milliliter of apoferritin solution. Successively, the pH was adjusted to 7.4 using 1 M NaOH. The resulting solution was stirred at room temperature for 2 h and then, after centrifugation, purified by gel filtration (superdex G25 column, Amersham) and dialysis. At the end of this process the concentrations of the protein (Bradford method, BSA standard), curcumin, and Gd were measured. The curcumin concentration has been measured spectrophotometrically at 430 nm in ethanol. Gd concentration was determined by using inductively coupled plasma mass spectrometry (ICP-MS; element-2; Thermo-Finnigan, Rodano (MI), Italy). Sample digestion was performed with concentrated HNO_3 (70%, 2 mL) under microwave heating (Milestone MicroSYNTH Microwave labstation). Size exclusion HPLC has been performed on an Alliance (Waters, USA) chromatographic system using a biosuite 450 column (Waters, USA). The column was calibrated with reference standard molecules (blue dextran molecular mass 2000 kDa, ferritin 450 kDa, thiroglobulin 669 kDa, catalase 232 kDa, and benzoic acid 122 Da, using the same buffer and experimental condition of the analytical runs. The calibration curve has been added as Supporting Information (Figure S1). The hydrated mean diameter and ζ potential of native apoferritin and of Apo-CUR-Gd preparations were determined using a Malvern dynamic light scattering spectrophotometer (Malvern Zetasizer 3000HS). All samples were analyzed at 25 °C in filtered (cutoff, 100 nm) HBS buffer (pH 7).

Animals. Eight-week-old (20–24 g of body weight) C57BL/6 male mice were used. The animals were housed in a controlled environment at a temperature of 22 ± 1 °C with a 12 h light–dark cycle. Food and water were provided *ad libitum*. The handling and all of the manipulations were carried out in accordance with the European Community guidelines, and allof the experiments were approved by the Ethical Committee of the University of Torino. Mice were divided into four groups. Group A (n = 7) received intraperitoneal (i.p.) thioacetamide (TA) 60 mg/kg; group B (n = 7) was pretreated 24 h before TA administration with Apo-CUR-Gd (63 mg/kg); group C (control; n = 3) received an equal volume of sterile 0.9% NaCl solution instead of TA, and group D (n = 3) received i.p. Gd-HPDO3A alone at the same dose administered to group B (0.007 mmol/kg). Finally, two further control groups of mice were used in the study: group E (n = 4) received i.p. native apoferritin alone (337 mg/kg of protein) 24 h before TA administration; group F (n = 4) received i.p. curcumin loaded apoferritin (without Gd-HPDO3A) (63 mg/kg of curcumin) 24 h before TA administration.

MR Images. MR images were acquired on a Bruker Avance 300 MHz spectrometer (7T) equipped with a Micro 2.5 microimaging probe (Bruker BioSpin, Ettlingen, Germany). The animals were anesthetized before MRI examination by intramuscle injection of tiletamine/zolazepam (20 mg/kg; Zoletil 100, Virbac, Milan, Italy) and xylazine (5 mg/kg; Rompun, Bayer, Milan, Italy). Apo-CUR-Gd (63 mg/kg of curcumin and 0.01 mmol/kg of Gd) was administered through i.p. injection. MR images were acquired before administration and after 1, 3, 5, and 24 h by using a T_1-weighted, fat-suppressed, spin–echo protocol (TR/TE/NEX = 250:3.2:6, FOV = 3 cm). The T_1 relaxation times of the different organs in the precontrast images were acquired by using a SNAPSHOT-FLASH sequence (TR/TE/NEX = 3.4:1.86:16). The mean signal intensity (SI)

dx.doi.org/10.1021/mp3006177 | *Mol. Pharmaceutics* 2013, 10, 2079–2085

values were calculated in the regions of interest drawn on the liver, muscle, spleen, and kidneys at all of the intervals when the MR images were acquired. The mean measured SI was normalized by using a standard solution of Gd in 1% HNO_3. The mean SI enhancement (%) of the target tissues was calculated according to eq 1:

$$\text{SI\% enhancement} = ((\text{mean SI}_{\text{POST}} - \text{mean SI}_{\text{PRE}}) / \text{mean SI}_{\text{PRE}}) \times 100 \quad (1)$$

Liver volumes were measured from T_2-weighted MRI images obtained by using a rapid acquisition with refocused echoes (RARE) sequence protocol (TR/TE/NEX = 8000:43:2).

Tissue Sample Handling. Twenty four hours after the TA injection, mice were anesthetized as for MRI analysis. Blood samples were drawn from the posterior cava vein for analysis of plasma ALT activity using a standard kit (Intrumentation Laboratory, Milano, Italy). Mice were then sacrificed by exsanguination, and fragments from the left lateral and middle lobes of the liver were obtained for histopathological assesment.

Histopathological Assesment. Fragments of 0.5 × 0.3 × 0.2 cm were fixed overnight in 4% buffered formaldehyde solution at 4 °C and processed by standard methods. Some 5 μm dewaxed sections stained with hematoxylin and eosin were used to evaluate the degree of damage. Injury was scored as follows: 0, no evidence of injury; 1, mild injury consisting in foci of hepatocytes with cytoplasmic vacuolar degeneration and clumped chromatin; 2, moderate injury consisting in foci of hepatocytes with cytoplasmic hypereosinofilia, loss of intercellular borders and nuclear pyknosis, and 3, severe injury consisting in coagulative necrosis with desintegration of hepatic cords, erythrocytes extravasation, and leucocytes infiltration. All evaluations were made on 10 nonconsecutive randomly chosen perivenular areas (magnification ×200).

Leukocytes Infiltration. Neutrophils and monocytes in the liver were quantitated in 10 nonconsecutive randomly chosen perivenular areas (magnification ×400).

Statistical Analysis. Data were expressed as means ± SEM (standard error of the mean) or ± SDM (standard deviation of the mean) as indicated in the different determinations. Statistical analyses were performed using the Student two-tailed *t* test. A *p* value less than 0.05 was considered statistically significant.

RESULTS AND DISCUSSION

Apo-CUR-Gd Preparation and Characterization. In the current study apoferritin is proposed as a curcumin delivery system. The encapsulation of curcumin in the apoferritin cavity has been followed by size exclusion chromatography by comparing the curves obtained at 215 and 430 nm, corresponding to the chromatograms of the protein and curcumin, respectively. A wavelength (λ) of 215 nm has been selected to monitor protein elution because at this λ apoferritin has a higher extinction coefficient (ε) than that measured at 280 nm. Figure 1A shows that after the dissociation/reassociation procedure the curcumin chromatographic peak (blue curve) has the same retention time of apoferritin (black curve). This demonstrates the colocalization of curcumin and the protein. Upon protein reassociation it is possible to observe an increase of a dimeric protein form (MW of about 860 kDa calculated from the column calibration curve reported in Figure S1, Supporting Information) that is already present in the native apoferritin solution (labeled with an asterisk). In order to rule out the possibility that after purification curcumin molecules remain

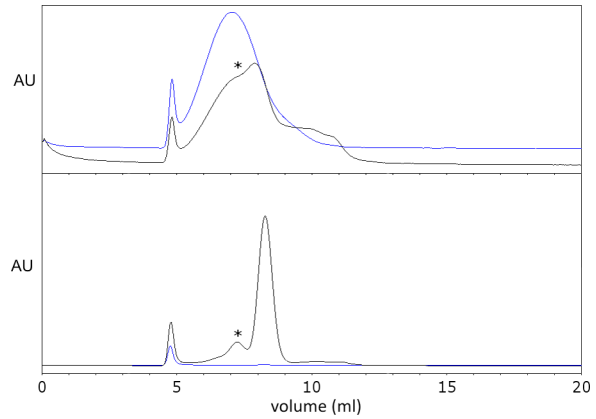

Figure 1. Size exclusion chromatograms. (A) Curcumin (blue) and apoferritin (black) chromatograms obtained after dissociation/reassociation procedure. (B) Curcumin (blue) and apoferritin (black) chromatograms obtained after 2 h incubation of the two compounds at pH = 7.4.

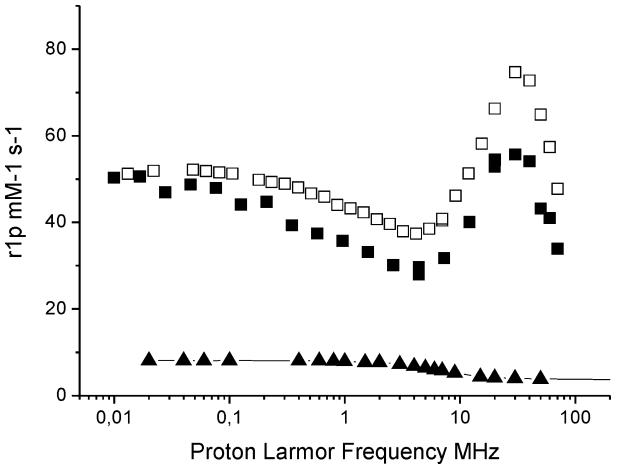

Figure 2. $1/T_1$ ^{1}H-NMRD profile (0.01−60 MHz; pH 7) and 25 °C of free Gd-HPDO3A (▲) compared with Gd-HPDO3A loaded apoferritin in the presence (■) or in the absence (□) of curcumin.

bound to the external protein surface, a second experiment was performed by incubating curcumin and apoferritin at room temperature and pH = 7.4 for 2 h without performing any dissociation/reassociation procedure. The chromatogram obtained at 430 nm (Figure 1B, blue line) shows the absence of a peak with the retention time of apoferritin. Only a small peak at low retention times (5 mL) is detectable corresponding to an impurity present also in the chromatogram of native apoferritin (Figure S2, Supporting Information). These observations allow us to rule out the occurrence of association of curcumin with the external surface of the protein as well as its diffusion through the apoferritin channels used by iron ions to form the iron oxide core inside the cavity. The binding to the protein surface is too weak to stabilize curcumin in water solution at neutral pH. The number of molecules per subunit that remained entrapped in the apoferritin (24 subunits/protein in the native form) upon the dissociation/reassotiation procedure is 9.5 ± 2 and 0.4 ± 0.1 for curcumin and Gd-HPDO3A, respectively. The hydrodynamic diameter of native apoferritin and Apo-CUR-Gd, measured by dynamic light scattering, were 11.9 ± 0.5 and 18.8 ± 1.8 nm, respectively. The increased hydrodynamic diameter of Apo-CUR-Gd with respect the native protein confirms its aggregation

dx.doi.org/10.1021/mp3006177 | *Mol. Pharmaceutics* 2013, 10, 2079−2085

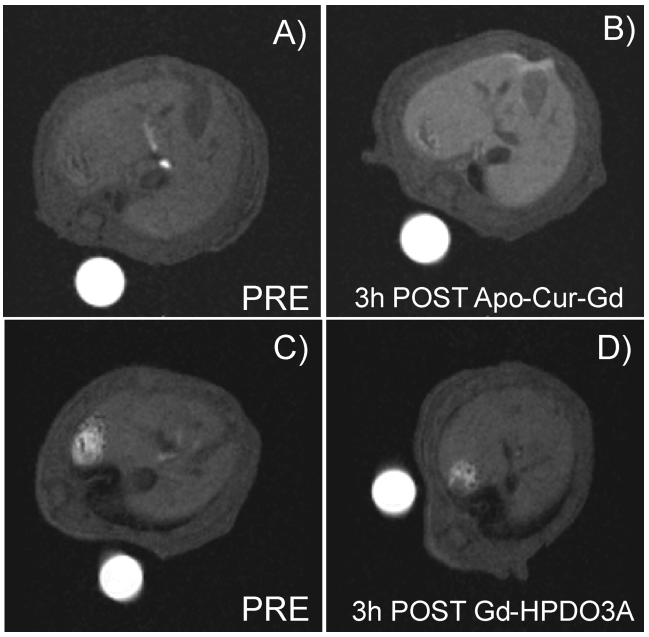

Figure 3. Fat-suppressed T_1-weighted MR spin−echo images (recorded at 7 T) of C57BL/6 mice liver, acquired before (A, C) and 3 h after the administration of Apo-CUR-Gd (B) and Gd-HPDO3A (D), respectively.

Table 1. % Signal Intensity Enhancements Measured 3 and 24 h after Contrast Administration Calculated Using the Equation Described in the Experimental Section. Data Are Expressed as Mean ± SDM

imaging probe	liver	muscle	kidneys	spleen
Apo-CUR-Gd 3 h	35 ± 8	1 ± 2	8 ± 4	21 ± 3
Apo-CUR-Gd 24 h	22 ± 6	0.8 ± 1	5 ± 2	9 ± 3
Gd-HPDO3A 3 h	4 ± 3	1 ± 2	6.5 ± 2	2 ± 1
Gd-HPDO3A 24 h	2 ± 1	0.7 ± 1	4 ± 2	1.5 ± 1

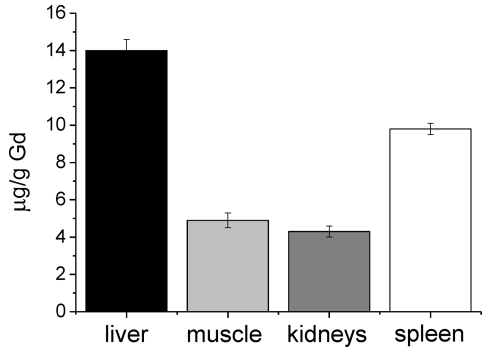

Figure 4. Gd concentration (μg/g) measured by ICP-MS in the different organs 3 h after the Apo-CUR-Gd administration.

during the dissociation/reassociation process. Native apoferritin and Apo-CUR-Gd ζ potentials were −4.6 ± 0.5 and −5.0 ± 0.6 mV, respectively.

Since the crucial point is to develop a delivery system able to protect curcumin from degradation, curcumin loaded apoferritin stability was assessed spectrophotometrically (430 nm) at 25 °C. In the first 2 h the absorbance shows a small decrease (15%) than it remains essentially constant during the entire experimental time (48 h). Without apoferritin more than 90% of curcumin decomposed rapidly (30′) in buffer at neutral pH as already reported by Zebib and co-workers.[9]

Apo-CUR-Gd ^{1}H Nuclear Magnetic Resonance Dispersion (NMRD) Profiles. As it has been previously reported,[2a] the paramagnetic complex inside the protein cavity shows a high millimolar relaxivity of 60−70 mmol/L^{-1} s^{-1} at 20 MHz and 25 °C, which is markedly higher than that observed in pure water (4.2 mM^{-1} s^{-1}). It has been shown that this outstanding relaxivity arises (i) from the interaction of the paramagnetic complex with the exchangeable protons (and likely the hydration water) on the protein surface of the apoferritin inner cavity[10] and (ii) from the increased reorientation time experienced by the complex in the inner protein cavity as a consequence of the increased viscosity.[11] The $1/T_1$ nuclear magnetic relaxation dispersion (NMRD) profile (Figure 2) of GdHPDO3A inside the apoferritin cavity is markedly higher than that for the free complex at any magnetic field strength with a relaxivity hump at ca. 1 T, as it is expected for macromolecular paramagnetic adducts endowed with slow molecular reorientational times. The copresence of curcumin does not produce significant changes in the paramagnetic properties of the complex inside the protein cavity.

***In Vivo* MRI and Apo-CUR-Gd Biodistribution.** In order to assess the potential of liver-targeted curcumin in protecting hepatocytes from acute injury, Apo-CUR-Gd has been tested in a murine model of acute hepatitis. TA administration is a well-documented strategy to develop acute liver injury in rodents.[12] TA is a potent acinar zone 3 toxicant, which undergoes a two-step bioactivation mediated by CYP2E1 to TA-sulfoxide and further to a reactive metabolite TA-S−S dioxide.[13] Consequently, the injured liver exhibits enhanced formation of reactive adducts, oxygen species, and lipid peroxides, stimulation of nuclear factor Kappa B, and the resultant expression of pro-inflammatory mediators.[14] Apo-CUR-Gd (63 mg/kg) was i.p. administered 24 h before the treatment with a toxic dose of TA (60 mg/kg). Drug uptake from the peritoneal cavity largely occurs through the portal circulation, therefore reducing systemic exposure and delivering almost all the compound directly into the liver.[15] Although apoferritin was from equine spleen, we did not expect any immunogenic reaction after a single i.p. administration of the compound in mice as a consequence of the extensive structural homology between mouse liver and horse spleen ferritins and apoferritins as judged by the similarity in the diffraction patterns of their crystals.[16] The Apo-CUR-Gd biodistribution was followed by MRI measuring the liver signal intensity enhancement in T_1-weighted images. The high relaxation enhancement efficiency of Gd complexes inside the cavity permits the detection of low concentrations of the imaging probe. Figure 3 shows the fat-suppressed T_1-weighted multislice spin−echo MR images obtained 3 h after the administration of the imaging probe. The SI enhancements measured in liver, kidney, spleen, and muscle (Table 1) evidenced the preferential uptake of Apo-CUR-Gd by the liver. Organ images are reported in Figure S3 (Supporting Information). The intraperitoneal i.p. injection of the same dose of free Gd-HPDO3A showed that the liver SI (Figure 3) remained unchanged as expected for this neutral and highly hydrophilic contrast agent whose excretion occurs only through the kidneys.[17] Fat-suppressed T_1-weighted MR spin−echo images of C57BL/6 mice liver, kidneys, and spleen acquired 24 h after the administration of Apo-CUR-Gd are reported in Figure S4 (Supporting Information). It is important to note that the observed MRI % SI enhancement shows that curcumin is still present in the liver at the time of thioacetamide administration (24 h after Apo-CUR-Gd injection)."

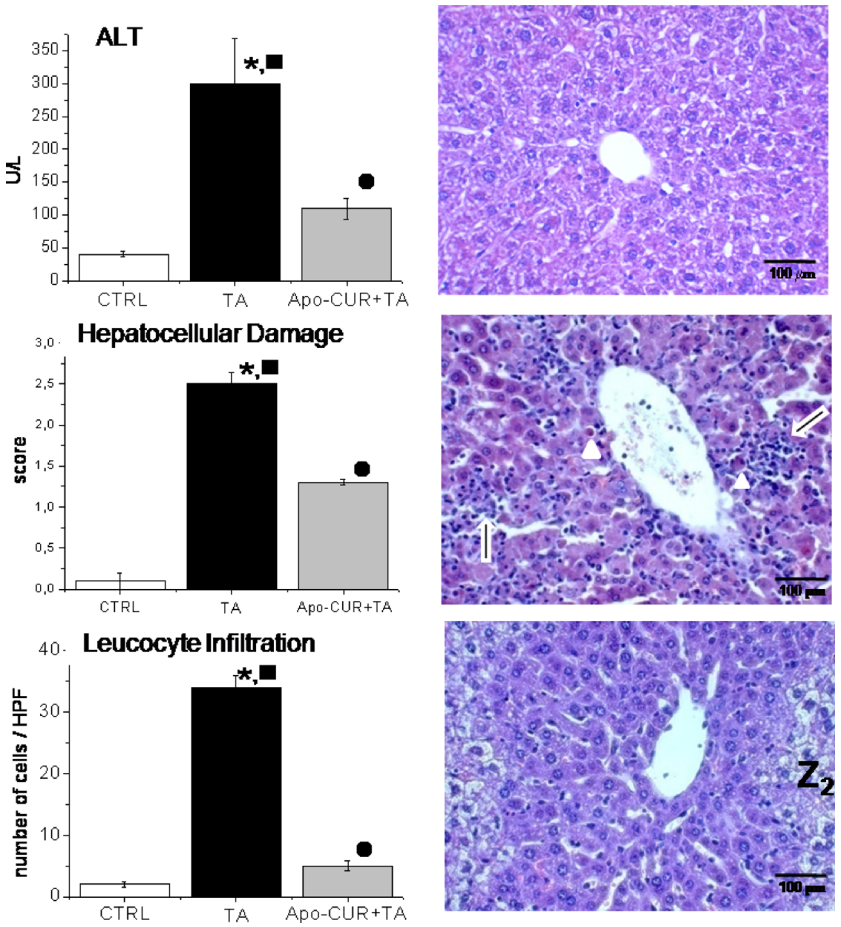

Figure 5. Parameters of liver injury after 24 h of TA challenge. ALT plasma activity: (*) TA vs CTRL (p = 0.01); (■) Apo-CUR-TA vs CTRL v(p = 0.005); (●) Apo-CUR + TA vs TA (p = 0.024). Hepatocellular score of damage: (*) TA vs CTRL (p = 0.0020); (■) Apo-CUR + TA vs CTRL (p = 0.0003); (●) Apo-CUR + TA vs TA (p = 0.0060). Leucocyte infiltration: (*) TA vs CTRL (p < 0.0001); (■) Apo-CUR + TA vs CTRL no significant; (●) Apo-CUR + TA vs TA (p < 0.0001). Data are expressed as means ± SE. Representative histological liver pictures from the CTRL (top level), TA (middle level), and Apo-CUR + TA (low level) mice are shown. Fields from the acinar zone 3 centered by a terminal hepatic venule were chosen. Top level: hepatocytes with a well-preserved cytoarchitecture; only some of them present scanty cytoplasmic fat microdoplets. Middle level: an extensive area of coagulative necrosis marked infiltrated by inflammatory cells is observed (arrow); occasional apoptotic bodies are also present (arrowhead). Low level: most of the perivenular hepatocytes appeared less damaged. To note, the inflammatory reaction is absent. At the transition with the acinar zone 2 (Z2), some hepatocytes show a moderate degree of hydropic degeneration, ($H/E \times 200$).

The millimolar concentration of the Apo-CUR-Gd in the liver was calculated from eq 2:

$$[\mathrm{Gd}] = (R_{1(\mathrm{post})} - R_{1(\mathrm{pre})})/r_{1\mathrm{p}} \quad (2)$$

The R_1 precontrast ($R_{1(\mathrm{pre})}$) maps were obtained by using a IR-SNAPSHOT-FLASH sequence.[18] R_1 postcontrast ($R_{1(\mathrm{post})}$) maps were calculated by using the pre- and postcontrast SI ratio (eq 3) calculated in the regions of interest, which were manually drawn on T_1-weighted images; $r_{1\mathrm{p}}$ is the relaxivity of Apo-CUR-Gd measured at 7 T (17.7 mM^{-1} s^{-1} at 7 T).

$$\begin{aligned} \mathrm{SI}_{(\mathrm{pre})}/\mathrm{SI}_{(\mathrm{post})} = {} & \{[1 - \exp((-\mathrm{TR} - \mathrm{TE})R_{1(\mathrm{pre})})] \\ & \times \exp(-\mathrm{TE} \times R_2)\} \\ & /\{[1 - \exp((-\mathrm{TR} - \mathrm{TE})R_{1(\mathrm{post})})] \\ & \times \exp(-\mathrm{TE} \times R_2)\} \end{aligned} \quad (3)$$

In eq 3,[19] TR represents the repetition time, TE is the echo time, and R_1 and R_2 are the longitudinal and transverse water proton relaxation times, respectively. By using an average curcumin/Gd ratio of 24, a liver curcumin concentration of about 0.7 ± 0.1 mM has been calculated. This concentration corresponds to ca. 19% of the administered dose (calculated using an average liver volume of 0.91 cm^3), and it is eight times higher than the amount found after the i.p. administration of a similar dose of curcumin alone dissolved in dimethyl sulfoxide.[20] The use of this theranostic agent permits us to evaluate in real time the drug concentration in the target organ thereby giving the possibility to adapt the therapeutic protocol to each patient individually. In order to confirm the contrast agent distribution obtained by MRI, the amount of Gd distributed in the different organs 3 h after the injection of Apo-CUR-Gd has been measured by ICP-MS on a forth group of mice (n = 4). Figure 4 shows that the Gd distribution (expressed as mg/g of tissue) in the different organs is the same of that obtained from the MRI signal intensity analysis (Table 1). The liver shows the highest Gd uptake, and the curcumin concentration estimated using the Gd concentration measured by ICP-MS (14 ug/g of Gd assuming a tissue density of 1 mg/mL) was of 2.1 mM. This value is three times higher than that estimated by MRI as a consequence of a lower Apo-CUR-Gd relaxivity observed upon internalization inside the hepatocytes. In fact, the internalization of MRI contrast agents

dx.doi.org/10.1021/mp3006177 | Mol. Pharmaceutics 2013, 10, 2079−2085

into cells can limit the attainable relaxation enhancement as a consequence of the reduced water exchange across the barriers among the different compartments.[21]

Hepatic Injury Evaluation. The extent of hepatic injury has been evaluated by measuring ALT activity in plasma and by histology assessment (Figure 5). In curcumin untreated animals TA caused an acute hepatitis. ALT activity increased ca. seven times with respect to control values (300 ± 69 vs 40 ± 4 U/L), and the histological evaluation showed a prominent acinar zone 3 necrosis with disorganization of the trabeculae architecture accompanied by an intense infiltration of inflammatory cells. Moreover, together with the irreversible damaged of the perivenular hepatocytes, occasional apoptotic bodies were also seen. A high ALT activity (270 ± 75 U/L), as well as a same extent of liver damage (Figure S4, Supporting Information) have been observed in mice pretreated with native apoferritin with the same protein dose used in the Apo-Cur-Gd (337 mg/kg), 24 h before TA administration. Livers preloaded with Apo-CUR-Gd were efficiently protected against the toxic action of TA. Clearly, the plasma level of ALT was attenuated to 110 ± 16 U/L (37% of curcumin untreated animals), and the necro-inflammation score was reduced to 1.3 ± 0.03 (52% of curcumin untreated animals). Hepatocytes appeared with a better preserved morphology, and the trabeculae integrity was maintained. Moreover, the degree of leukocyte infiltration was drastically reduced as well as the presence of apoptotic cells (Figure 5). Curcumin administration was previously shown to be hepatoprotective in liver injuries caused by carbon tetrachloride, trichloroethylene, endotoxin, ethanol, and TA,[4] but to the best of our knowledge, this is the first report where liver protection was achieved by means of a theranostic agent able to deliver curcumin selectively into the hepatocytes. Because of the multiple pharmacological actions of curcumin, it is difficult to determine which of them mediated the above-described therapeutic effect. It is well-understood that, as a consequence of liver damage, intracellular components are released from necrotic cells. Such molecules are able to alarm and activate the local immune cells triggering reactive oxygen species mediated killing process which leads to apoptosis, oncosis-necrosis, and consequently an amplified harmful inflammatory reaction. Since Apo-CUR-Gd pretreatment nearly turned-off the inflammatory cells recruitment, we propose that the obtained protection could be mediated by regulation of stress-signaling pathways redox-dependent involved in the release of alarmins and the expression of pro-inflammatory mediators. The same results have been obtained treating mice with curcumin loaded apoferritin (without Gd-HPDO3A) administered 24 h before TA treatment (ALT activity = 103 ± 12 U/L), thus indicating the same therapeutic efficacy in the absence of Gd.

■ CONCLUSIONS

Apoferritin can be considered as an efficient carrier for therapeutics and probes for imaging guided treatment of a variety of liver diseases. The encapsulation of curcumin inside the apoferritin cavity significantly increases its stability and bioavailability while maintaining its therapeutic antioxidant and anti-inflammatory properties.

■ ASSOCIATED CONTENT

Supporting Information

Figure S1 showing Biosuite 450 column calibration curve. Figure S2 showing gel filtration chromatogram of native apoferritin. Figure S3 showing T_1-weighted MR images of C57BL/6 mice kidneys, spleen, and intestine acquired 3h after the administration of Apo-CUR-Gd. Figure S4 showing T_1-weighted MR images of C57BL/6 mice liver, kidneys, and spleen acquired before and 24h after the administration of Apo-CUR-Gd . Figure S5 showing a representative histological liver picture from mice pretreated with native apoferritin 24h before TA administration. This material is available free of charge via the Internet at http://pubs.acs.org.

■ AUTHOR INFORMATION

Corresponding Author

*Fax: +39 011 6706487; e-mail: simonetta.geninatti@unito.it.

Author Contributions

J.C.C. and S.G.C. contributed equally.

Notes

The authors declare no competing financial interest.

■ ACKNOWLEDGMENTS

This research was performed in the framework of the EU COST Action TD1004, "Theranostics Imaging and Therapy: an Action to Develop Novel Nanosized Systems for Imaging-Guided Delivery" and supported by Regione Piemonte (PIIMDMT), and nano-IGT projects), MIUR (PRIN 2009235JB7), ENCITE-project (FP7-HEALTH-2007A), and Consorzio Interuniversitario di Ricerca in Chimica dei Metalli dei Sistemi Biologici (CIRCMSB)

■ REFERENCES

(1) (a) Geninatti Crich, S.; Cutrin, J. C.; Lanzardo, S.; Conti, L.; Kálmán, F. K.; Szabó, I.; Lago, N. R.; Iolascon, A.; Aime, S. Mn-loaded apoferritin: a highly sensitive MRI imaging probe for the detection and characterization of hepatocarcinoma lesions in a transgenic mouse model. *Contrast Media Mol. Imag.* **2012**, *7* (2), 81−8. (b) Huang, J.; Zheng, D. L.; Qin, F. S.; Cheng, N.; Chen, H.; Wan, B. B.; Wang, Y. P.; Xiao, H. S.; Han, Z. G. Genetic and epigenetic silencing of SCARA5 may contribute to human hepatocellular carcinoma by activating FAK signaling. *J. Clin. Invest.* **2010**, *120*, 223−41. (c) Makino, A.; Harada, H.; Okada, T.; Kimura, H.; Amano, H.; Saji, H.; Hiraoka, M.; Kimura, S. Effective encapsulation of a new cationic gadolinium chelate into apoferritin and its evaluation as an MRI contrast agent. *Nanomed. Nanotechnol. Biol. Med.* **2011**, *7*, 638−646.

(2) (a) Aime, S.; Frullano, L.; Geninatti Crich, S. Compartmentalization of a gadolinium complex in the apoferritin cavity: a route to obtain high relaxivity contrast agents for magnetic resonance imaging. *Angew. Chem., Int. Ed. Engl.* **2002**, *41*, 1017−9. (b) Geninatti Crich, S.; Bussolati, B.; Tei, L.; Grange, C.; Esposito, G.; Lanzardo, S.; Camussi, G.; Aime, S. Magnetic resonance visualization of tumor angiogenesis by targeting neural cell adhesion molecules with the highly sensitive gadolinium-loaded apoferritin probe. *Cancer Res.* **2006**, *66*, 9196−201.

(3) (a) Lammers, T.; Rizzo, L. Y.; Storm, G.; Kiessling, F. Personalized nanomedicine. *Clin. Cancer Res.* **2012**, *15*, 4889−94. (b) Lammers, T.; Aime, S.; Hennink, W. E.; Storm, G.; Kiessling, F. Theranostic Nanomedicine. *Acc. Chem. Res.* **2011**, *44*, 1029−38. (c) Lammers, T.; Kiessling, F.; Hennink, W. E.; Storm, G. Nanotheranostics and image-guided drug delivery: current concepts and future directions. *Mol. Pharmaceutics* **2010**, *7*, 1899−912. (d) Janib, S. M.; Moses, A. S.; MacKay, J. A. Imaging and drug delivery using theranostic nanoparticles. *Adv. Drug Delivery Rev.* **2010**, *62*, 1052−63.

(4) Rivera-Espinoza, Y.; Muriel, P. Pharmacological actions of curcumin in liver diseases or damage. *Liver Int.* **2009**, *29*, 1457−1466.

(5) (a) Shapiro, H.; Ashkenazi, M.; Weizman, N.; et al. Curcumin ameliorates acute thioacetamide-induced hepatotoxicity. *J. Gastroenter. Hepatol.* **2006**, *21*, 358−366. (b) Reyes-Gordillo, K.; Segovia, J.; Shibayama, M.; et al. Curcumin prevents and reverses cirrhosis induced by bile duct obstruction or CCl4 in rats: role of TGF-beta modulation and oxidative stress. *Fundam. Clin. Pharmacol.* **2008**, *22*, 417−427. (c) Shishodia, S.; Singh, T.; Chaturvedi, M. M. Modulation of

transcription factors by curcumin. *Adv. Exp. Med. Biol.* **2007**, *595*, 127−148.
(6) NCI. Clinical development plan: curcumin. *J. Cell Biochem.* **1996**, *26S*, 72−85.
(7) Zhang, F.; Koh, G. Y.; Jeansonne, D. P.; Hollingsworth, J.; et al. A novel solubility-enhanced curcumin formulation showing stability and maintenance of anticancer activity. *J. Pharm. Sci.* **2011**, *100*, 2778−89.
(8) (a) Yallapu, M. M.; Jaggi, M.; Chauhan, S. C. Curcumin nanoformulations: a future nanomedicine for cancer. *Drug Discovery Today* **2012**, *17*, 71−80. (b) Basnet, P.; Hussain, H.; Tho, I.; Skalko-Basnet, N. Liposomal delivery system enhances anti-inflammatory properties of curcumin. *J. Pharm. Sci.* **2012**, *101*, 598−609.
(9) Zebib, B.; Mouloungui, Z.; Noirot, V. Stabilization of curcumin by complexation with divalent cations in glycerol/water system. *Bioinorg. Chem. Appl.* **2010**, *2010*, 292760.
(10) Vasalatiy, O.; Zhao, P.; Zhang, S.; Aime, S.; Sherry, A. D. Catalytic effects of apoferritin interior surface residues on water proton exchange in lanthanide complexes. *Contrast Media Mol. Imag.* **2006**, *1*, 10−14.
(11) Fries, P. H.; Belorizky, E. Enhancement of the water proton relaxivity by trapping Gd3+ complexes in nanovesicles. *J. Chem. Phys.* **2010**, *133*, 024504.
(12) (a) Eder, M.; Butenandt, O.; Joster, R. Morphologic, histochemical and autoradiographic studies on acute and chronic thioacetamide poisoning. *Frankf Z. Pathol.* **1965**, *74*, 599−619. (b) Trennery, P. N.; Waring, R. H. Early changes in thioacetamide-induced liver damage. *Toxicol. Lett.* **1983**, *19*, 299−307.
(13) Chilakapati, J.; Shankar, K.; Korrapati, M. C.; et al. Saturation toxicokinetics of thioacetamide: role in initiation of liver injury. *Drug Metab. Dispos.* **2005**, *33*, 1877−1885.
(14) Park, J. H.; Kum, Y. S.; Lee, T. L.; et al. Melittin attenuates liver injury in thioacetamide-treated mice through modulating inflammation and fibrogenesis. *Exp. Biol. Med. (Maywood)* **2011**, *236*, 1306−1313.
(15) Markman, M. Intraperitoneal antineoplastic drug delivery: rationale and results. *Lancet Oncol.* **2003**, *4*, 277−283.
(16) Rice, D. W.; et al. Structural homology between mouse liver and horse spleen ferritins. *FEBS Lett.* **1985**, *181*, 165−168.
(17) Eakins, M. N.; Eaton, S. M.; Fisco, R. A.; et al. Physicochemical properties, pharmacokinetics, and biodistribution of gadoteridol injection in rats and dogs. *Acad. Radiol.* **1995**, *2*, 584−91.
(18) Deichmann, R.; Haase, A. Quantification of T1 values by SNAPSHOT-FLASH NMR Imaging. *J. Magn. Reson.* **1992**, *96*, 608−612.
(19) Shiftan, L.; Israely, T.; Cohen, T.; Frydman, V.; Dafni, H.; Stern, R.; Neeman, M. Magnetic resonance imaging visualization of hyaluronidase in ovarian carcinoma. *Cancer Res.* **2005**, *65*, 10316−10323.
(20) Goel, A.; Kunnumakkara, A.; Aggrarwal, B. B. Curcumin as "Curecumin": from kitchen to clinic. *Biochem. Pharmacol.* **2008**, *75*, 787−809.
(21) (a) Kok, M. B.; Hak, S.; Mulder, W. J.; van der Schaft, D. W.; Strijkers, G. J.; Nicolay, K. Cellular compartmentalization of internalized paramagnetic liposomes strongly influences both T1 and T2 relaxivity. *Magn. Reson. Med.* **2009**, *61*, 1022−32. (b) Terreno, E.; Geninatti Crich, S.; Belfiore, S.; Biancone, L.; Cabella, C.; Esposito, G.; Manazza, A. D.; Aime, S. Effect of the intracellular localization of a Gd-based imaging probe on the relaxation enhancement of water protons. *Magn. Reson. Med.* **2006**, *55*, 491−7.